Vol.66: e23230556, 2023
https://doi.org/10.1590/1678-4324-2023230556
ISSN 1678-4324 Online Edition

Article - Engineering, Technology and Techniques

Development of an Acoustic Test Bench for Fault Localization in Gas Insulation Substations

Diogo Gonzaga Marcelo[1]
https://orcid.org/0000-0002-5832-9402

Ronny Francis Ribeiro Junior[1]
https://orcid.org/0000-0003-0244-3553

Júlio Cezar Oliveira Castioni[2]
https://orcid.org/0000-0002-1144-9247

Mateus Mendes Campos[1]
https://orcid.org/0000-0002-8654-1048

Clailton Leopoldo da Silva[2]
https://orcid.org/0000-0001-7840-0352

Isac Antônio dos Santos Areias[1]
https://orcid.org/0000-0003-4562-5285

Rafael Martins[2]
https://orcid.org/0000-0002-0776-2978

Frederico de Oliveira Assunção[1]
https://orcid.org/0000-0002-5304-8628

Germano Lambert-Torres[1]*
https://orcid.org/0000-0003-3789-4696

Luiz Eduardo Borges da Silva[1]
https://orcid.org/0000-0003-2298-1017

[1]Instituto Gnarus, Itajubá, Minas Gerais, Brasil; [2]COPEL Geração e Transmissão, Curitiba, Paraná, Brasil.

Editor-in-Chief: Alexandre Rasi Aoki
Associate Editor: Alexandre Rasi Aoki

Received: 27-May-2023; Accepted: 10-Jul-2023

*Correspondence: germanoltorres@gmail.com; Tel.: +55-35- 3622-0132 (G.L.T.).

HIGHLIGHTS

- Development of an acoustic test bench to reproduce of GIS features.
- The proposed approach includes traveling waves and triangulation methods.
- The proposed approach can detect short-circuit and partial discharges.
- It is useful to detect early disturbance in the substation.

Abstract: Shielded substations with SF6 gas insulation (GIS) play a critical role in supplying power to urban areas, and it is crucial to quickly identify and isolate faults to restore system operation and meet supply demands. However, locating faults in such substations can involve extensive and time-consuming procedures, such as opening and closing hermetically sealed compartments containing SF6. This paper presents the development of an acoustic test bench that accurately replicates the dynamic characteristics of SF6 shielded substations. By utilizing the traveling wave technique, partial discharges occurring in high-voltage insulation can be detected and precisely located. The method employs various techniques, including the analysis of the arrival time of traveling waves at different points within the substation and triangulation methods. The use of traveling waves in partial discharge detection offers several advantages, such as precise fault location and non-interference with normal substation operations. Additionally, acoustic methods are highly sensitive to other sources of partial discharges, such as moving particles and fluctuating potential discharges. The results demonstrate that the combination of the acoustic test bench and the disturbance localization technique presents an innovative approach to fault location studies in GIS. The acoustic test

bench enables controlled simulation of failure conditions, providing accurate data on the acoustic behavior of substations. Through the disturbance location technique, these data can be analyzed and interpreted to pinpoint the exact fault location. This integrated approach enhances the efficiency of the troubleshooting process and reduces the time required to repair GIS.

Keywords: gas insulated substation; partial discharge; acoustic methods; traveling waves.

INTRODUCTION

The importance of a substation for the functionality of electrical networks and the continuation of its services is the driving force behind this research effort [1]. Due to their location in key urban areas for the delivery of energy, armored substations with SF6 gas insulation (GIS) near the major consumption centers must ensure a high level of operational reliability [2, 3].

Therefore, when a problem occurs in a substation, shutdowns occur that need to be logged, identified, and isolated in order to allow the substation to be reconfigured as quickly as possible. In this way, it will be able to resume its operation and restore the largest possible amount (or even all) of the energy necessary to supply the system's demands. The time needed to identify the problem spots (or failures) is one of the major challenges that causes this recovery procedure to take longer [4].

This fault identification procedure is essential to the recovery of the substation. There are specific problems that can happen in a substation whose nature is clear-cut, allowing for speedy localization. For instance, flashover in insulator chains or defects in machinery where the protection is functioning as intended reveals the faulty circuit (or machinery), the troubled area, or even the location of the fault. When a transformer has an internal defect and the differential protection operates as intended, this occurs. In this instance, the equipment where the fault occurred is known, and it must be taken out during the substation's restoration operation. The major issue is when the substation's current protection mechanisms fail to work as intended [4].

It is typical to find a high percentage of wrong actions or refusals to act during the commissioning phase of substations or even in substations that are already in operation, especially those of a more complex constructive and operational characteristic [5]. Due to the requirement to evaluate huge amounts of data in these substations, identifying problems brought on by protection sensors that behave inappropriately typically takes a long time. This happens because supplementary protections, which grow the damaged region and make it challenging to locate the defective circuit (or equipment), can disguise the failure under certain circumstances. The system setup, the kind and level of safeguards, event records, oscillograms, and other data are some of the things that need to be studied [6].

When working with outdoor substations, it is crucial to keep in mind that a visual examination is typically required in the substation yard [7]. Even though this inspection can take a while, especially in big substations, it can aid in the identification of faults. It is substantially more challenging to locate faults in this kind of substation because this element does not apply to armored substations with SF6 gas insulation [8].

Operators are currently responsible for fault detection and determining the sources and effects of malfunctions. Unfavorable outcomes could happen if any of these tasks are incorrectly carried out [9, 10]. Furthermore, the wrong placement of a malfunction in a substation of this kind necessitates substantial repair carried out by numerous experts. When choosing the compartment in which work is to be done, a variety of steps need to be carried out because the circuits are kept in hermetically sealed compartments with SF6. These steps entail taking the SF6 gas out of the compartment, opening it up to make any necessary repairs, shutting it up, putting new SF6 gas in it, and checking the compartment's seal. It is crucial to keep in mind that these processes take time, and tests may require more time than actual problem correction [11]. Given that, all the steps must be taken to open and close the compartment, taking a significant amount of time to complete, without an effective solution to the problem, we can now imagine the inconvenience (in terms of time and cost) that an incorrect location of the faulty compartment can cause.

The development of an acoustic test bench for identifying fault events in armored substations with SF6 gas insulation is addressed in this paper. The system, which included noise creation in the interior and surface, was constructed with a shielded tubular pipe hermetic to SF6. This laboratory configuration, referred to as a reduced model lab, replicates the important dynamic properties.

The method for detecting partial discharges in GIS (gas insulated substations) using traveling waves and the acoustic methods used in this study are presented in next section. The bench built for the laboratory of acoustic techniques used to find partial discharges in GIS is then described. The tests performed on the GIS test bench, including the frequency test and fault location, are presented in the next section. The mechanical

disturbance fault location system is then presented together with the mathematical tools that were used, and the tests and outcomes of the application of disturbances on the test bench are finally shown in the sequence.

Detections of partial discharges by traveling waves in GIS

When a change, such as a disturbance, occurs in a certain area of the GIS system, it may spread to other areas by means of moving or mechanical waves. These progressive mechanical waves in an elastic medium are related to the transmission of energy, not matter, from one point to another in the medium. Other phenomena are produced by this propagation, with reflections, refractions, interferences, and diffractions being the most prevalent ones [12, 13].

Partial discharge (PD) detection in GIS substations (gas insulated substations) is a critical problem to guarantee the safety and dependability of these high-voltage systems. To identify and localize these incomplete discharges, the traveling-wave approach has been frequently used. In this paper, we will show how to apply this strategy to the detection of partial discharges in GIS using relevant data.

Partial discharges are electrical events caused by faults in high-voltage insulation, such as air bubbles, foreign particles, or insulating material failures. These discharges can prematurely age insulation and, in extreme cases, trigger catastrophic collapse. As a result, identifying and localizing these discharges is crucial for minimizing system damage and downtime [14]. Methods involving detection using electromagnetic and acoustic waves stand out among the conceivable applications based on the idea of traveling waves.

Electromagnetic methods applied in the detection of partial discharges in GIS

The traveling wave approach takes advantage of electromagnetic waves' characteristics as they move via cables and transmission lines. An electromagnetic wave is formed and propagates across the system when a partial discharge occurs at a point in the GIS substation. This wave can be detected and analyzed to detect partial discharges [14, 15].

Several techniques based on the traveling wave method are employed in the detection of partial discharges. Analyzing the waveforms produced by partial discharges is a frequent approach. The waves are captured with sensors like antennas or probes, then processed and evaluated. The amplitude, length, and frequency of these waveforms are evaluated to determine the presence and location of partial discharges [16].

Another approach is to examine the arrival times of traveling waves at various points across the substation. Signals collected at various sites are compared, and the time difference between them is utilized to predict the location of partial discharges. This method necessitates a precise synchronization system to enable accurate arrival time measurements [17]. Furthermore, the traveling wave method can be combined with other detection techniques, such as frequency analysis and wavelet transformation, to improve the accuracy and reliability of the results [18].

The use of traveling waves to detect partial discharges in GIS has various advantages. For example, this approach pinpoints partial discharges, allowing for focused and effective correction actions. Furthermore, the detection of partial discharges based on traveling waves is non-invasive; that is, it does not necessitate the suspension of normal substation operations [15].

Electromagnetic (EM) waves associated with partial discharges (PD) begin to propagate within a GIS section shortly after a partial discharge pulse is activated due to abnormalities in an internal insulating material. Part of the energy is wasted during this process in the form of radio waves with a steep wavefront [19- 21]. Traveling waves can be reduced, degraded, or modified due to environmental variables, external interferences, and surrounding elements such as the structure of the GIS.

As the partial discharge (PD) signal propagates through the medium, such as the dielectric gas and insulating spacers, there is a reduction in its intensity. The attenuation caused by dielectric gases, such as sulfur hexafluoride (SF6), has a minimal impact on the signal since the attenuation coefficient usually varies between 3-5 dB/km [22] and can reduce the propagation speed of the EM wave between 2.10^8 m/s and $2.3.10^8$ m/s [23].

It is crucial to note, however, that the insulating spacers found in GIS substations have a substantial impact on the partial discharge (PD) signal as it travels through them. In general, passing through the insulating spacers results in a 3 dB reduction in signal power intensity [24].

Acoustic methods applied in the detection of partial discharges in GIS

Acoustic partial discharges are like "micro sparking." As the gas returns to the evacuated partial discharge channel, an acoustic shock wave is generated, traveling from the PD location across the surrounding GIS structure [25].

Acoustic approaches are frequently sensitive enough to detect partial discharge sources such as moving particles, fluctuating potential discharges, and bumps, especially when they emit detectable sounds. However, because these materials exhibit high degrees of attenuation to acoustic signals, it is often rather difficult to locate sources of partial discharges in solid dielectrics, such as voids or weak surface discharges, using acoustic techniques. In any case, substantial amounts of pre-amplification are commonly required to pick up the signals. In general, partial discharge acoustic detection systems rely on piezoelectric sensors fitted to the GIS housing and coupled to an instrument designed for this purpose. Piezoelectric sensors (acoustic emission sensors, accelerometers, or condenser microphones used to pick up acoustic signals from partial discharges) typically operate in the frequency range of hundreds of hertz to several hundred kHz (maximum 1 MHz). Some typical examples of piezoelectric sensors are shown in Figure 1.

Most important work in establishing the methodologies and effectiveness of acoustic techniques for diagnosing partial discharges in gas-insulated systems (GIS) was done in the 1990s [25–32] and continues presently [33, 34].

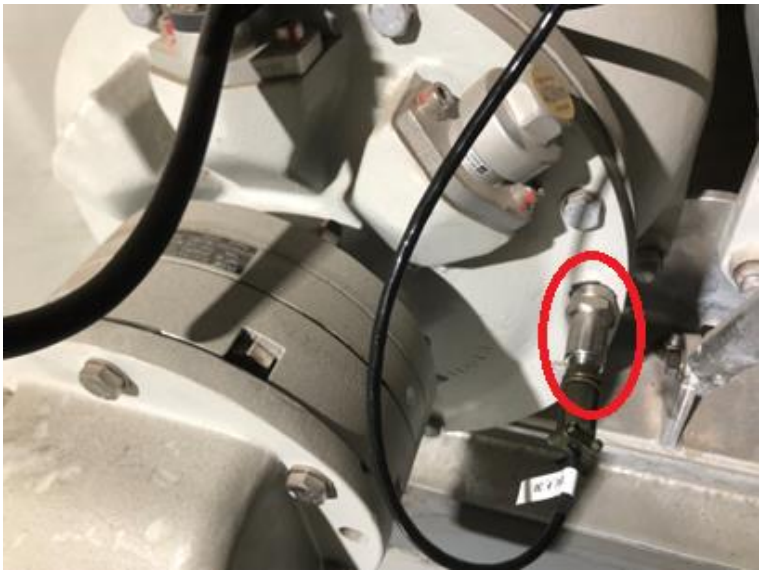

Figure 1. Piezoelectric acoustic sensors.

Particularly compared to radiofrequency techniques used externally on SF6 pipes, the acoustic methodology for detecting partial discharges in GIS substations has significant advantages. First, the acoustic technique is less expensive since it does not necessitate the installation of new equipment or complex signal transmission systems. Acoustic detection uses piezoelectric acoustic sensors, which are relatively inexpensive and can be simply added to existing GIS cabinets without requiring any structural alterations [25].

Furthermore, the acoustic technique is less invasive because it does not require SF6 duct entry to detect incomplete discharges. While radiofrequency techniques necessitate the placement of external antennas or electromagnetic field sensors around the GIS structure, the acoustic method employs piezoelectric sensors that are mounted directly to the cabinets. This eliminates the need to disrupt routine substation operations and reduces the danger of system component damage [25].

When detecting partial discharges, the acoustic technique outperforms radiofrequency techniques applied externally to SF6 pipelines. Piezoelectric sensors have a high sensitivity for capturing acoustic signals created by partial discharges, especially when the discharges produce signals of sufficient amplitude. This enables more accurate and reliable fault identification, particularly in settings where partial discharge sources are difficult to detect using existing techniques [35].

In summary, the utilization of the acoustic approach, used in the laboratory, offers substantial advantages over radiofrequency techniques applied externally to the SF6 pipelines. This method is less expensive, less invasive, and more sensitive, providing a cost-effective and dependable option for monitoring partial discharges in high-voltage systems.

Laboratory of acoustic methods applied in the detection of partial discharges in GIS

The description of the building of the acoustic test bench, shown in Figure 2, will be described in this section, along with the specifics and features of the material manufacturing process. The goal of designing the acoustic test system is to allow for the monitoring and localization of fault events in SF6 shielded substations. This system is made up of shielded and hermetic tube structures, as shown in Figure 3, that may generate noise in various interior positions and perform surface measurements.

Based on this approach, the reduced model laboratory is a dynamic environment in which experiments are carried out. In addition to acoustic noise measurements, the system provides connection of gas, allowing for the creation of a vacuum inside the structure and the pressurization of it as necessary. These properties provide a diverse and adequate laboratory setting for investigations linked to the detection and location of failure occurrences in SF6 shielded substations, allowing for a variety of tests and controlled simulations under specified conditions.

As a result, the designed acoustic test system has the capability of simulating and analyzing breakdown events in armored substations in a precise and controlled manner. The combination of hermetic isolation and noise creation in various positions enables a complete examination of the acoustic properties of these occurrences, which contributes to the development of more efficient and reliable detection and localization systems. The ability to generate diverse internal pressure and vacuum conditions broadens the study possibilities, allowing for the evaluation of the system's behavior in various operational settings.

This experimental approach, which makes use of an acoustic test bench, is critical for furthering knowledge in the field of faults in SF6 shielded substations, giving significant data for the enhancement of monitoring and diagnostic systems, and thereby adding to the safety and dependability of these systems.

Figure 2. Reduced model lab.

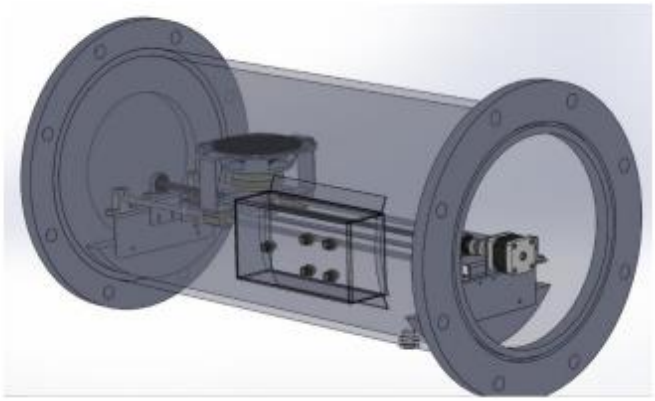

Figure 3. Reduced model lab GIS compartment.

Figure 4 shows the test system, which is made up of armored piping. This piping, made of 304 stainless steel, resembles an armored substation. In the reduced model lab, each unit of armored tubing is 3/8" thick and has an outside diameter of 272mm. Five identical, 500-mm-long devices were produced. These

machines have gas connections, allowing for pressurization, vacuum, and the installation of sensors to monitor the SF6 gas quality. When remotely actuated, the static and dynamic parts within the armored pipe emit sound, imitating normal operation or breakdowns. This system architecture enables accurate and controlled testing and experiments in the smaller model laboratory.

Figure 4. Reduced Model Laboratory pipelines.

The internal component layout was carefully engineered to ensure that the loudspeaker goes perfectly across the whole duct compartment without compromising the seal. The motor, speakers, guides, spindle, inductive sensors, mounts, and connectors were all strategically configured for the project, as shown in Figure 5. This method enables fitting the application's specific needs while ensuring the system's appropriate and efficient operation.

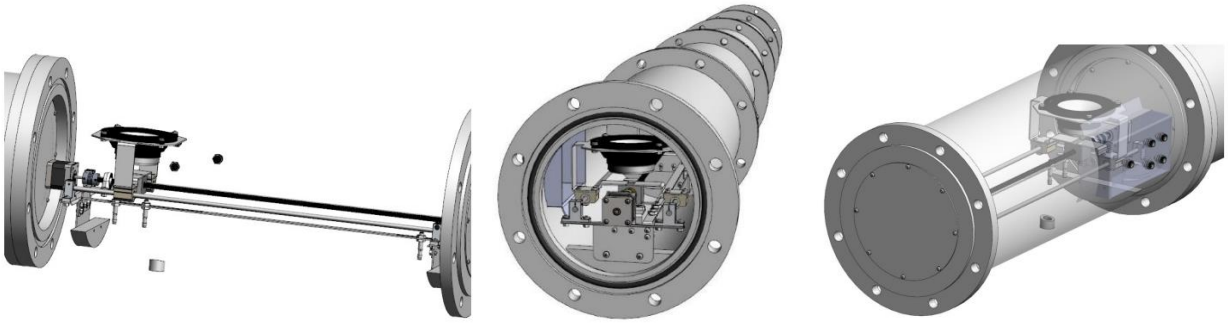

Figure 5. Internal, front, and external view of the components that make up the test bench.

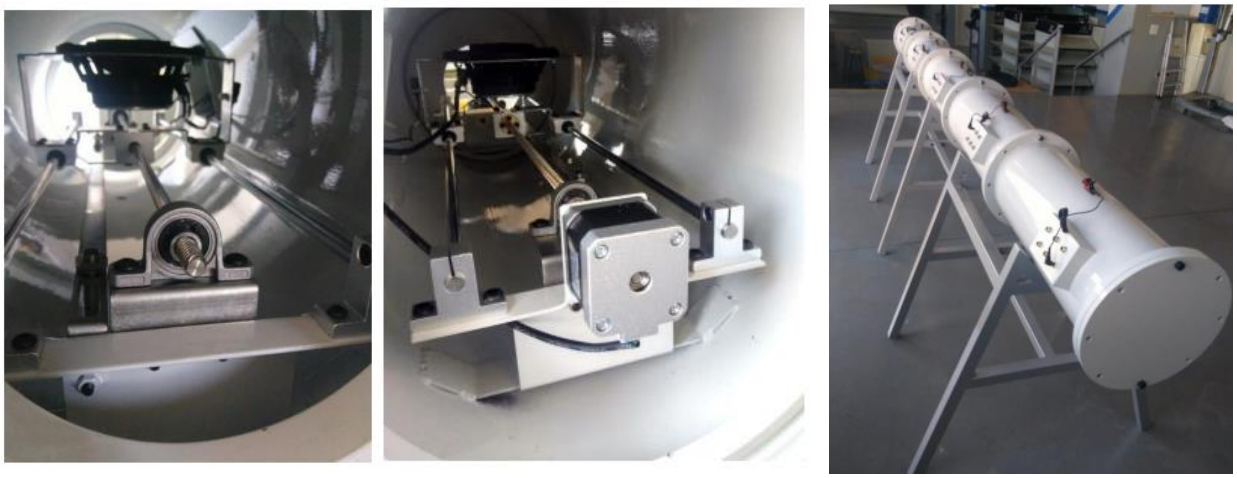

Figure 6. Installation of the motor, microphone and cables and assembly of the final test bench.

The guides, spindles, and speaker bracket were precisely fitted into the ducts in their correct positions during bench construction. The stepper motor was then connected to the trapezoidal spindle, and an internal microphone was attached on the speaker support's side. The cables were connected to the ducts via the necessary connectors. Figure 6 show the procedure of situating the ducts on their supports, as well as the ducts during assembly, with the contact microphone fitted into its connector.

Tests with the GIS Test BENCH

The results of the tests performed on the GIS test bench are reported in this section. Several criteria were analyzed, and key concepts were validated, in preparation for the development of the concept prototype.

The objective of the frequency test was to verify the speaker's responsiveness to emitting noise at a predetermined frequency. For this, an internal microphone and an external microphone were used to compare the signal strength across the spectrum.

The loudspeaker emitted a steady sinusoidal signal with a frequency of 1200 Hz in the first test. The microphones are arranged as shown in Figure 7, with the lavalier microphone near the loudspeaker and the contact microphone located outside the duct. The contact microphone's exterior position makes it impossible to catch the transmitted signal.

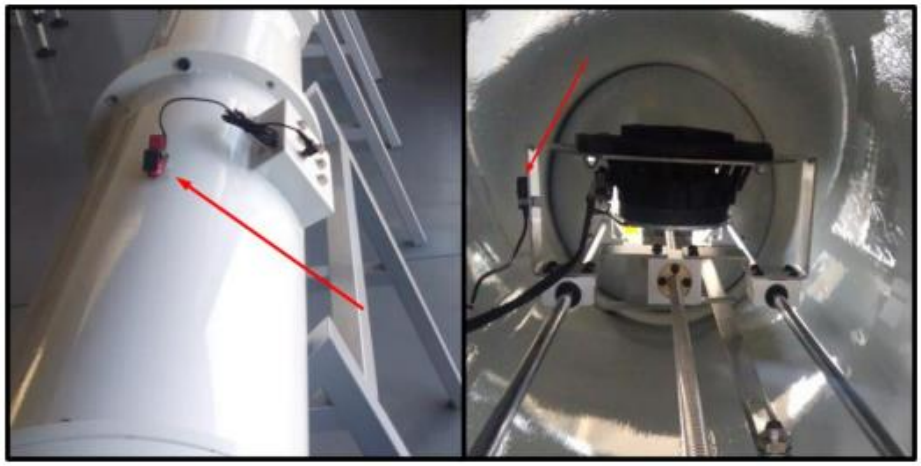

Figure 7. Left: Contact microphone location. Right: Lavalier microphone location.

Figures 8 and 9 show the data obtained from the spectrograms acquired by the microphones. Figure 8 spectrogram clearly shows that the spectral component with the greatest strength corresponds to the frequency of 1,200 Hz, as expected. Figure 9 shows a high intensity in the range of 1,200 Hz; however, there is a difference in intensity in the signals at other frequencies. This variation is due to the pickup properties of the microphones utilized. The signal is received by the contact microphone through the vibration of the material in contact, making it susceptible to reflections and other disturbances in the environment.

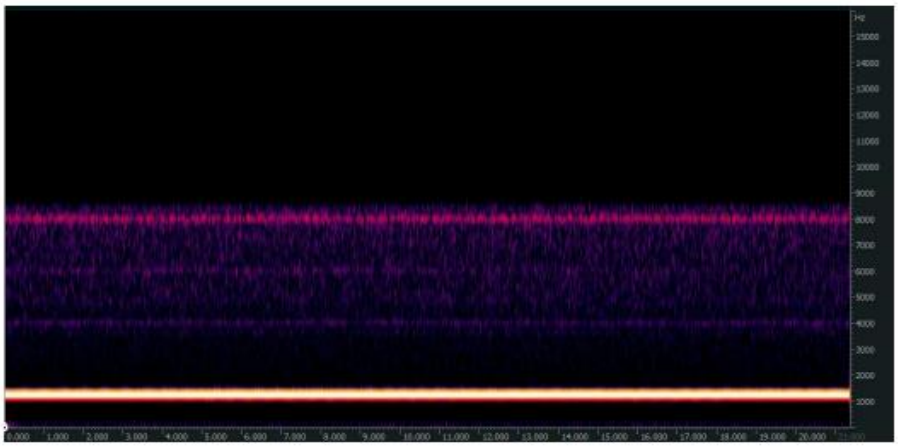

Figure 8. Internal microphone 1.2kHz signal spectrogram.

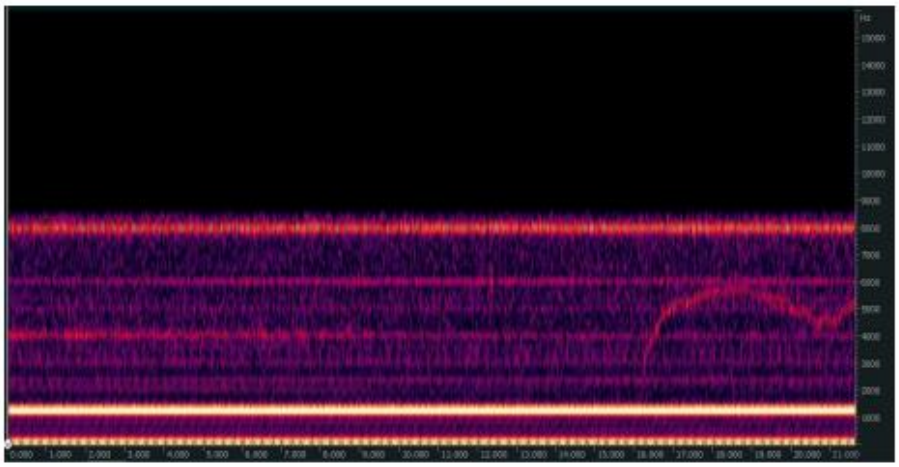

Figure 9. Spectrogram of the external microphone's 1.2kHz signal.

Fault location system due to mechanical disturbance

The localization system is comprised of two major components: hardware and software. The hardware consists of an acoustic sensor system (such as accelerometers) and a signal collection system specialized in obtaining the signals acquired by the acoustic sensors. The software is responsible for analyzing the information from the acoustic sensors to locate the fault that originated from the GIS substation. The schematic diagram of the fault location system is shown in Figure 10.

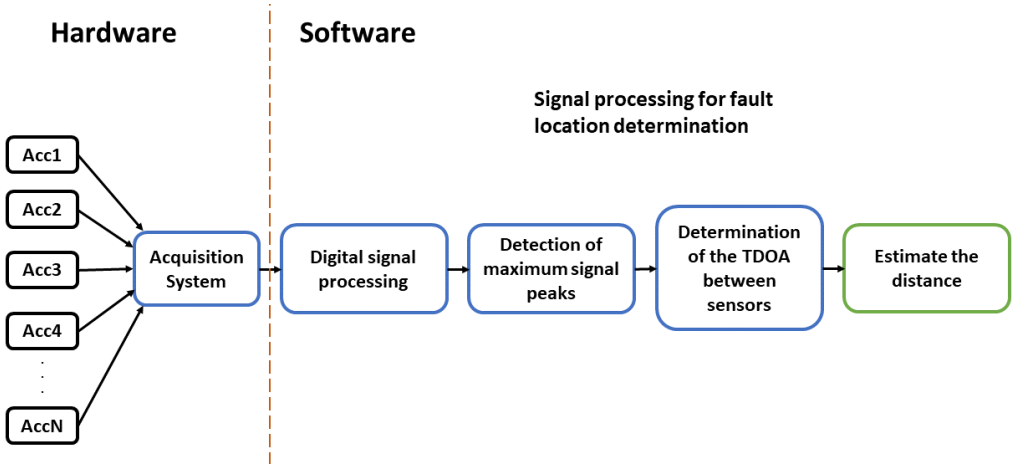

Figure 10. Schematic diagram of the fault location system.

A axial sensor with output type with a sensitivity of 100 mV/g, a dynamic range of 80g, and an application range of 0.6 Hz to 15 kHz were employed in the GIS reduced model laboratory for disturbance localization experiments. For the laboratory experiments, four accelerometers of this type were placed in the ducts at specific locations.

A power supply and signal conditioning equipment for the accelerometers are connected to an analog-digital conversion system in the acquisition system. The ADC system features a configurable sample frequency and bit resolution. It contains communication software that allows it to make digital signals available in binary or CSV formats.

The digital signal processing applied to accelerometer digital signals consists of the use of band-pass-type digital filters within the accelerometer's operating band, with a lower cutoff frequency of 200 Hz and an upper cutoff frequency of 25 kHz.

The software detects the greatest peaks of the accelerometer signals after the signals have been processed. The greatest peaks of the signals are critical for establishing the first detection zones. As a result, the accelerometer with the greatest amplitude incidence is closest to the failure event, and the second accelerometer with the greatest peak value defines the section where the likely failure is located.

After locating the largest peaks of each signal, the algorithm proceeds to process the flight times (arrival times, ToF). After threshold applications, signal flight durations are determined by detecting oscillation peaks [36]. The algorithm determines a threshold level, and after the signal exceeds the expected level, the

algorithm begins to process the values of the times when the signal oscillation peaks. Differences in arrival times (TDOA, or time difference of arrival) are calculated between pairs of two accelerometers by subtracting the ToF values determined by each accelerometer [37]. For the location of the detected events, the concepts of the arrival time difference principle are used. Figure 11 shows an example of TDOA in the pipeline.

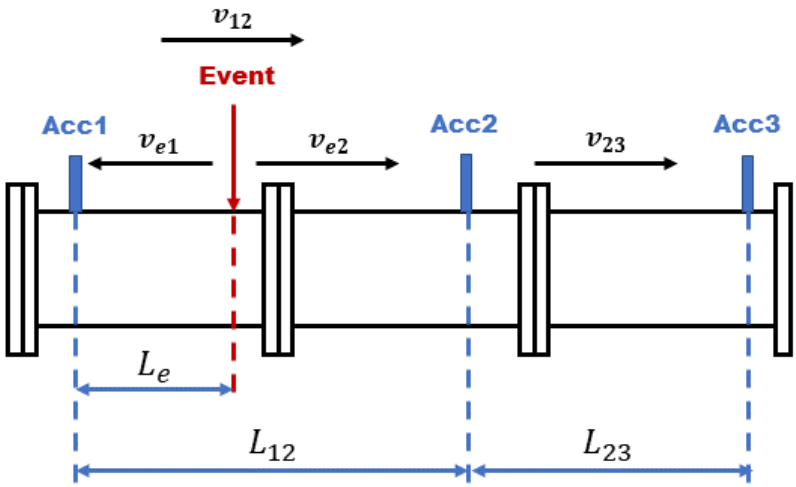

Figure 11. Example of TDOA in the pipeline.

Observing Figure 11, when an event (or fault) occurs between two accelerometers, the maximum amplitude of accelerometer 1 (Acc1) will be higher than that of accelerometer Acc2 which, in turn, will be greater than accelerometer Acc3, indicating that the fault is between the first two accelerometers. The fault will generate an acoustic signal that will propagate in two different directions, with velocity v_{e1} in the direction of the accelerometer 1 and v_{e2} in the direction of the accelerometer 2. Therefore, the estimated time between the difference in arrival times on the accelerometers will have a value Δt_{12_e} in section 1-2 of the event. Thus, they must $\Delta t_{12_e} < L_{12}/v_{12}$, that is, the TDOA obtained will be smaller than the natural ratio of a single velocity propagation direction (v_{12}). Based on this and following the literature [37], these relationships are obtained for the event presented:

$$L_e = \frac{L_{12} - V.\Delta t_{12_e}}{2},$$

Where, L_e is the distance from the fault to the accelerometer with the highest amplitude peak (in the case of the example Acc1) in meters; L_{12} represents the distance between the two accelerometers of greater amplitude in meters; V is the apparent speed of the traveling wave emitted by the event in a direction of propagation in m/s; Δt_{12_e} is the arrival time difference between the two accelerometers in seconds. The velocity V can be approximated for a second set of accelerometers that have a single direction of propagation, so for the example $V \cong v_{23}$ or $V \cong L_{23}/\Delta t_{23}$.

FAULT LOCATION TESTS AND RESULTS

Four accelerometers were strategically placed in the reduced model laboratory to conduct the localization experiment. Figure 12 depicts the respective positions of the accelerometers. Table 1 displays the distances associated with the positioning of the accelerometers in the simplified model.

Table 1. Distances relative to accelerometer placements.

Acronym	Distance [meters]
1-2	1.38
1-3	1.96
1-4	2.69
2-3	0.58
2-4	1.31
3-4	0.73
POINT 1 – ACC01	0.23

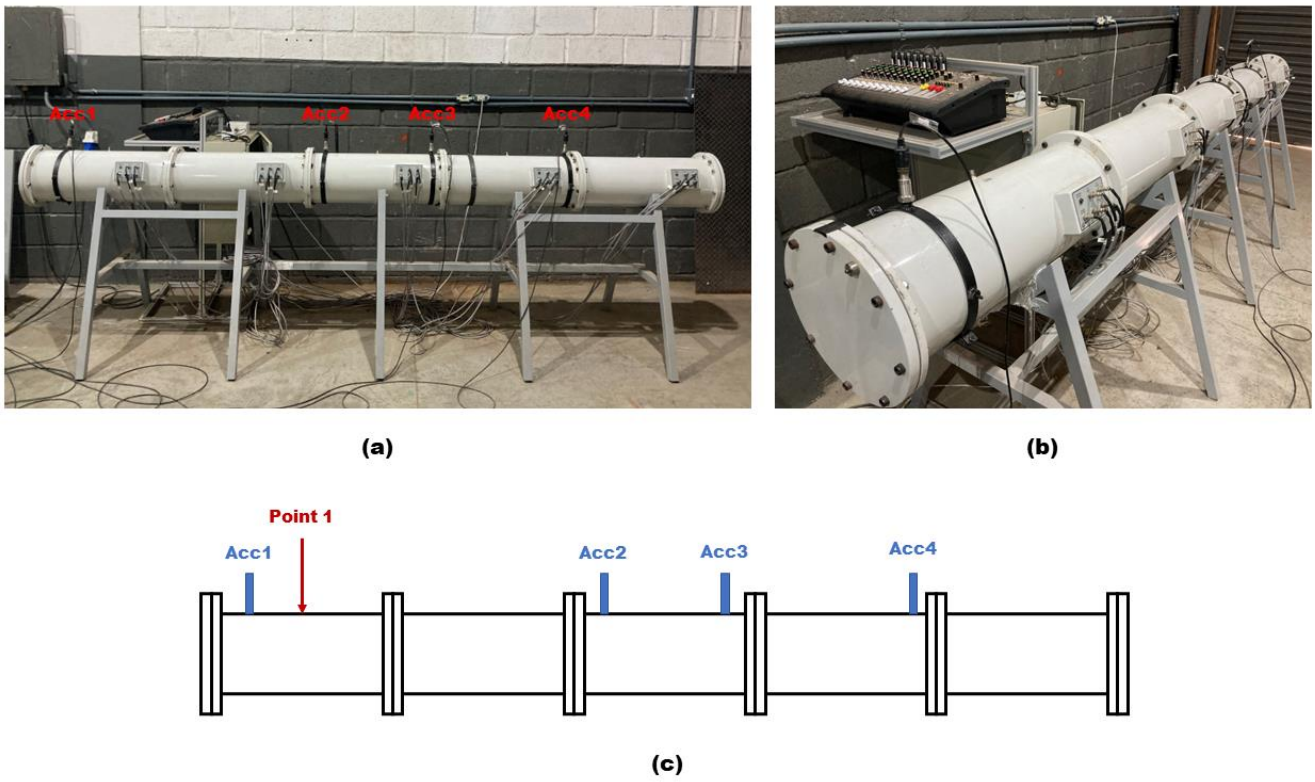

Figure 12. Reduced model laboratory: (a) Accelerometer positions physically; (b) Second view of the positioning of the accelerometers; and (c) Point of event.

A vibration event was simulated in the reduced laboratory conduit using an impact hammer. As shown in Table 1 and Figure 12, the impact point is positioned between accelerometers 1 and 2, at 23 cm from accelerometer 1. In the chosen region, a total of ten impact events were executed, with data captured by the acquisition system and processed to determine location by the location processing algorithm.

Amplitude of acquired signals

The fault position detection algorithm is used after obtaining data for the ten impact occurrences at the test location. Figure 13 shows an acquisition made via the acquisition system.

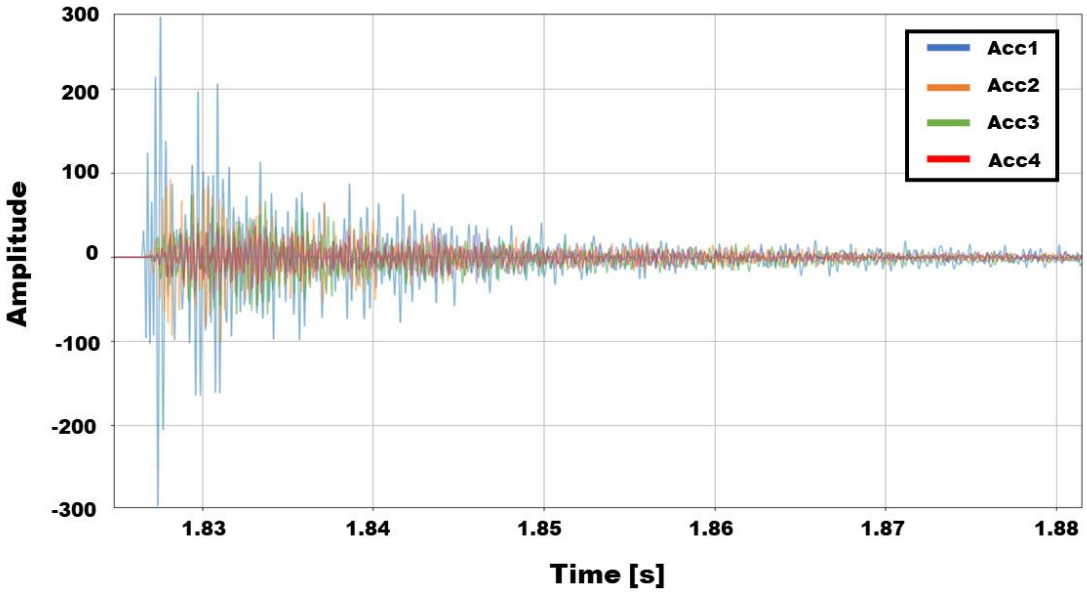

Figure 13. Acquisition performed by the acquisition system.

The signal amplitude of accelerometer 1 is greater than that of the others, confirming that the event is closer to accelerometer 1. The intensity of the second accelerometer is greater than the intensity of the other two, indicating that the failure is between accelerometers 1 and 2.

Time Difference of Arrival (TDOA)

The processing determines the differences in time of flight (time difference of arrival) between pairs of accelerometers. The data obtained are presented in Table 2.

Table 2. The ToF differences for the ten acquisitions.

Measurements	TDOA determined between two accelerometers					
	1-2	1-3	1-4	2-3	2-4	3-4
1	3.26507E-04	5.02461E-04	7.85373E-04	2.05364E-04	4.78514E-04	2.60412E-04
2	3.48119E-04	5.04095E-04	7.98261E-04	2.22764E-04	4.87125E-04	2.58120E-04
3	3.23380E-04	4.88140E-04	7.89853E-04	2.22758E-04	4.97323E-04	2.53857E-04
4	3.07135E-04	4.94551E-04	7.91489E-04	2.21545E-04	4.78479E-04	2.62107E-04
5	2.91476E-04	4.85940E-04	7.99924E-04	2.11279E-04	4.75203E-04	2.60091E-04
6	2.98500E-04	4.72958E-04	7.78385E-04	2.23608E-04	4.53377E-04	2.60618E-04
7	3.21176E-04	5.23781E-04	7.95415E-04	2.15783E-04	4.84354E-04	2.66237E-04
8	3.26417E-04	4.98032E-04	8.10893E-04	2.16380E-04	4.43841E-04	2.60718E-04
9	3.44846E-04	5.16596E-04	7.91439E-04	2.14305E-04	4.60837E-04	2.66795E-04
10	3.24374E-04	5.27157E-04	7.95390E-04	2.16861E-04	4.66197E-04	2.54729E-04
MEAN	**3.21193E-04**	**5.01371E-04**	**7.93642E-04**	**2.17065E-04**	**4.72525E-04**	**2.60368E-04**
STD	**1.81065E-05**	**1.72745E-05**	**8.75341E-06**	**5.84937E-06**	**1.63727E-05**	**4.19379E-06**

Determination of the apparent speeds of the signals

Once differences in arrival times have been measured, the apparent velocity of the sound waves traveling throughout the laboratory can be calculated. Table 3 shows the estimated apparent velocities between the accelerometers.

The average apparent speeds in segments 2-3, 2-4, and 3-4 are 2673.79, 2775.37, and 2804.37 [m/s], respectively. These estimated apparent velocities have just one direction of sound wave propagation, whereas the values of the other pairs (1-2, 1-3, and 1-4) present two directions of sound wave propagation from the impact event.

Table 3. Apparent speed estimates

Measurements	Apparent velocities on the stretches between the accelerometers					
	1-2	1-3	1-4	2-3	2-4	3-4
1	4226.55	3900.80	3425.12	2824.25	2737.64	2803.25
2	3964.17	3888.16	3369.83	2603.65	2689.25	2828.14
3	4267.42	4015.24	3405.70	2603.73	2634.10	2875.63
4	4493.14	3963.19	3398.66	2617.98	2737.84	2785.13
5	4734.53	4033.42	3362.82	2745.19	2756.72	2806.71
6	4623.12	4144.13	3455.87	2593.82	2889.43	2801.03
7	4296.70	3742.02	3381.88	2687.88	2704.63	2741.91
8	4227.71	3935.49	3317.33	2680.47	2951.51	2799.96
9	4001.79	3794.07	3398.87	2706.42	2842.65	2736.18
10	4254.35	3718.06	3381.99	2674.52	2809.97	2865.79
MEAN	**4308.95**	**3913.46**	**3389.81**	**2673.79**	**2775.37**	**2804.37**
STD	**246.13**	**134.80**	**37.31**	**73.32**	**97.36**	**45.18**

Estimation of distances by TDOA

Applying the theory described in Section 5, the distance values of the impact event are obtained (Point 1). Table 4 presents the distance estimates from the point of impact in relation to accelerometer 1.

Table 4. Estimates of distances from the point of impact to the accelerometer 1.

Measurements	Estimated Distance by TDOA between accelerometers		
	1-2	**1-3**	**1-4**
1	0.243	0.292	0.270
2	0.222	0.302	0.272
3	0.264	0.337	0.305
4	0.270	0.303	0.262
5	0.288	0.310	0.242
6	0.259	0.296	0.221
7	0.256	0.272	0.269
8	0.208	0.245	0.148
9	0.200	0.246	0.220
10	0.234	0.275	0.228
MEAN	**0.244**	**0.288**	**0.244**
STD	**0.028**	**0.029**	**0.043**

The calculated distances in the three sections are 0.244, 0.288, and 0.244 meters, respectively, with an overall average of 0.259 meters. When we compare the estimated values to the numbers in Table 4, we get the relative deviations given in Table 5.

Table 5. Relative deviations.

Acronym	Estimated distances [meters]	Distance from Acc1 to Point 1 [meters]	Absolute deviation [meters]	Relative deviation [%]
1-2	0.244	0.230	0.014	6.1
1-3	0.288	0.230	0.058	25.2
1-4	0.244	0.230	0.014	6.1
MEAN	0.259	0.230	0.029	12.6

The results show that the bench designed for simulating disturbances in GIS substations can find disturbances using accelerometers on its surface, making it a viable choice for testing this non-invasive monitoring technology with low implementation costs. Furthermore, this monitoring technique is an appealing choice for GIS substations that were installed without a monitoring system and may be indicating the presence of a disturbance, necessitating the zoning of candidate compartments in order to carry out some form of repair.

CONCLUSIONS

Fault location in armored substations with SF6 gas insulation is a challenging operation that necessitates extensive information and time analysis. Detecting these failures becomes considerably more difficult when protection measures fail, making it difficult to identify the defective circuit or equipment. Furthermore, the time required for interventions is increased by the essential processes, such as the removal of SF6 gas and leak checks. The created acoustic test bench, on the other hand, represents a potential method for studying failure event locations in SF6 armored substations.

The developed bench simulates the essential dynamic features of substations in a laboratory setting using the traveling wave method. Bench tests that do frequency analysis and fault detection are useful for detecting and pinpointing partial discharges. Partial discharge detection is critical for ensuring the safety and reliability of GIS substations. In this case, the traveling wave approach allows the localization of partial discharges without interfering with the substation's routine activities during detection. The technique used on the acoustic test bench was able to localize the disturbances using only the accelerometer data, based on

the results of the disturbance localization tests. This location technology enables faster and more effective interventions, minimizing substation downtime and boosting overall electrical system reliability.

Funding: The projects presented in this paper are part of the R&D project PD-06491-0513-2018, executed by Gnarus Institute for COPEL Generation and Transmission, under the Brazilian Electric Sector Research and Development Program, regulated by the National Electric Energy Agency (ANEEL).
Acknowledgments: The authors would like to express their thanks to CNPq, and CAPES**.**
Conflicts of Interest: The authors declare no conflict of interest**.**

REFERENCES

1. Areias IAS, Borges da Silva LE, Bonaldi EL, de Lacerda de Oliveira LE, Lambert-Torres G, Bernardes VA. Evaluation of Current Signature in Bearing Defects by Envelope Analysis of the Vibration in Induction Motors. Energies. 2019;12(21):4029. doi: 10.3390/en12214029.
2. Marmonter J, Villard V, Hossenlopp L, Garg RK. Increasing availability of GIS installations by using digital control, protection and monitoring systems. Proceedings of the 2000 IEEE Power Engineering Society Winter Meeting. 2000 Jan 23-27; Singapure. Piscataway (NJ): IEEE; c2000 p. 2055-61. doi: 10.1109/PESW.2000.847670.
3. Dos Reis JO, da Silva CL, Assunção FO, Castioni JCO, Martins R, Xavier CE, Areias IAS, Junior RFR, Lambert-Torres G, Bonaldi EL, da Silva LEB, Oliveira LEL. On the use of vibration analysis for contact fault detection in high-voltage HVCBs. Braz Arch Biol Tech. 2023; 66: e23230286. doi: 10.1590/1678-4324-2023230286.
4. Halpin SM, Jones RA, Taylor LY. The MVA-Volt Index: A Screening Tool for Predicting Fault-Induced Low Voltage Problems on Bulk Transmission Systems. IEEE Trans Pow Syst. 2008 Aug; 23(3):1205-10. doi: 10.1109/TPWRS.2008.926405.
5. Padilla E. Substation automation systems: design and implementation. Hoboken (NJ): John Wiley & Sons; c2015. 272 p.
6. Yao Y, Wang N. Fault diagnosis model of adaptive miniature circuit breaker based on fractal theory and probabilistic neural network. Mech Syst Sign Proc. 2020 Aug; 142: 106772. doi: 10.1016/j.ymssp.2020.106772.
7. Liu J, Zhao Z, Ji J, Hu M. Research and application of wireless sensor network technology in power transmission and distribution system. Intell Conv Netw. 2020 Sept; 1(2): 199-220. doi: 10.23919/ICN.2020.0016.
8. Prabakaran T, Powl J, Uppili B. PD test in gas insulated substation using UHF method. Proceedings of the 2015 International Conference on Condition Assessment Techniques in Electrical Systems. 2015 Dec 10-12; Bangalore, India. Piscataway (NJ): IEEE; c2015 p. 57-60. doi: 10.1109/CATCON.2015.7449508.
9. Sant'Ana WC, Lambert-Torres G, Bonaldi EL, Gama BR, Zacarias TG, Areias IAS, Arantes DA, Assuncao FO, Campos MM, Steiner FM. Online Frequency Response Analysis of Electric Machinery through an Active Coupling System Based on Power Electronics. Sensors. 2021; 21(23), 8057. doi: 10.3390/s21238057.
10. Da Silva CL, Reis O, Assuncao FO, Castioni JCO, Martins R, Xavier CE, et al. An Online Non-Invasive Condition Assessment Method of Outdoor High-Voltage SF6 Circuit Breaker. Machines. 2023; 11(3): 323. doi:10.3390/machines11030323.
11. Wölke B, Ramesh M, Schneider AC, Jebamony D. Pilot of an environmentally friendly SF6-free MV switchgear technology and assessment of sensor technologies. Proceedings of the 25th International Conference on Electricity Distribution. 2019 Jun 3-6; Madrid, Spain. Paris: CIRED; c2019 p. 1-5. doi: 10.34890/757.
12. Achenbach J. Wave propagation in elastic solids. Amsterdam: North Holland; 1973. 440 p.
13. Okubo H, Beroual A. Recent Trend and Future Perspectives in Electrical Insulation Techniques in Relation to Sulfur Hexafluoride (SF6) Substitutes for High Voltage Electric Power Equipment. IEEE Elect Ins Mag. 2011 Mar-Apr; 27(2): 34-42. doi: 10.1109/MEI.2011.5739421.
14. Haque SM, Rey JAA, Masúd AA, Umar Y, Albarracin R. Electrical properties of different polymeric materials and their applications: The influence of electric field. In: Du B, editor. Polymer Dielectrics. Amsterdam: InTech; 2017. p.41-63. doi: 10.5772/67091
15. Okabe S, Kaneko S, Yoshimura M, Muto H, Nishida C, Kamei M. Partial discharge diagnosis method using electromagnetic wave mode transformation in gas insulated switchgear. IEEE Trans Diel Elect Ins. 2007 Jun; 14(3): 702-9. doi: 10.1109/TDEI.2007.369534.
16. Alvarez F, Ortego J, Garnacho F, Sanchez-Uran MA. A clustering technique for partial discharge and noise sources identification in power cables by means of waveform parameters. IEEE Trans Diel Elect Ins. 2016 Feb; 23(1):469-81. doi: 10.1109/TDEI.2015.005037.
17. Alvarez F, Ortego J, Garnacho F, Sanchez-Uran MA. Application of HFCT and UHF sensors in on-line partial discharge measurements for insulation diagnosis of high voltage equipment. Sensors. 2015; 15(4) 7360-87. doi: 10.3390/s150407360.
18. Aftab MA, Hussain SMS, Ali I, Ustun TS. Dynamic protection of power systems with high penetration of renewables: A review of the traveling wave based fault location techniques. Int J Elect Pow En Syst. 2020 Jan; 114: 105410. doi: 10.1016/j.ijepes.2019.105410.
19. Koch HJ, Gas Insulated Substations. Hoboken (NJ): John Wiley & Sons; c2014. 496 p.

20. Kaneko S, Okabe S, Muto H, Yoshimura M, Nishida C, Kamei M. Electromagnetic wave radiated from an insulating spacer in gas insulated switchgear with partial discharge detection. IEEE Trans Diel Elect Ins. 2009 Feb; 16(1): 60-8. doi: 10.1109/TDEI.2009.4784552.
21. Lozano-Claros D, Custovic E, Elton D. Two planar antennas for detection of partial discharge in gas-insulated switchgear (GIS). Proceedings of the 2015 IEEE International Conference on Communication, Networks and Satellite. 2015 Dec 10-12; Bandung, Indonesia. Piscataway (NJ): IEEE; c2015 p. 8-15, doi: 10.1109/COMNETSAT.2015.7434301.
22. Hoshino T, Nojima K, Hanai M. Real-time PD identification in diagnosis of GIS using symmetric and asymmetric UHF sensors. IEEE Trans Pow Del. 2004 Jun; 19(3): 1072-7. doi: 10.1109/TPWRD.2003.822944.
23. Jung SY, Kim JY, Oh CS, Lee BW, Koo JY. Measurement of propagation velocity of the electromagnetic wave produced by partial discharge in a gas-insulated switchgear. Proceedings of the Telecommunications Energy Conference. 2009 Oct 18-22; Incheon, South Korea. Piscataway (NJ): IEEE; c2009. p. 1-7, doi: 10.1109/INTLEC.2009.5351889.
24. Kurrer R, Feser K. The application of ultra-high-frequency partial discharge measurements to gas-insulated substations. IEEE Trans Pow Del. 1998 Jul; 13(3): 777-82. doi: 10.1109/61.686974.
25. Behrmann G, Koltunowicz W, Schichler U. State of the Art in GIS PD Diagnostics. Proceedings of the 2018 Condition Monitoring and Diagnosis (CMD). 2018 Sept 23-26; Perth, Australia, Piscataway (NJ): IEEE; c 2018. pp. 1-6. doi: 10.1109/CMD.2018.8535741.
26. Lundgaard LE. Partial Discharge - Part XIV: Practical Application. IEEE Elect Ins Mag. 1992 Sep-Oct; 8(5): 34-43. doi: 10.1109/57.156943.
27. CIGRE WG 15.03. Effects of Particles on GIS and the Evaluation of Relevant Diagnostic Tools. Paris: CIGRE; Report 15-103, 1994. 11p.
28. Lundgaard LE. Partial Discharge - Part XIII: Acoustic Partial Discharge Detection - Fundamental Considerations. IEEE Elect Ins Mag. 1992 Jul-Aug; 8(4): 25-31. doi: 10.1109/57.145095.
29. CIGRE JWG 33/23.12. Insulation Co-ordination of GIS: Return of Experience, On Site Tests and Diagnostic Techniques. Electra. 1998 Feb; 176: 67-97.
30. Leijon M, Vlastos A. Pattern Recognition of Free Metallic Particles Motion Modes in GIS. Proceedings of the 1988 IEEE International Symposium on Electrical Insulation. Cambridge, MA. Piscataway (NJ): IEEE; c1998. p. 120-3. doi: 10.1109/ELINSL.1988.13883.
31. Bargigia A, Koltunowicz W, Pigini A. Detection of parallel discharges in gas insulated substations. IEEE Trans Pow Del. 1992 Jul; 7(3): 1239-49. doi: 10.1109/61.141837.
32. Lundgaard LE. Particles in GIS Characterization from Acoustic Signatures. IEEE Trans Diel Elect Ins. 2001 Dec; 8(6): 1064-74. doi: 10.1109/94.971466.
33. IEC TS 62478. High-voltage Test Techniques – Measurement of Partial Discharge by electromagnetic and acoustic Methods. Geneva, Switzerland: IEC Press. 2016. 42 p.
34. CIGRE WG D1.37. Guidelines for Partial Discharge Detection using conventional (IEC 60270) and unconventional Methods. CIGRE Technical Brochure No. 662. Paris: CIGRE. 2016. 115 p.
35. Dai K, Liao Y. A novel system and experimental verification for locating partial discharge in gas insulated switchgears. Int J Emerg Elect Pow Syst. 2019; 20(2): 0277. doi: 10.1515/ijeeps-2018-0277.
36. Yang F, Shi D, Lo LY, Mao Q, Zhang J, Lam KH. Auto-Diagnosis of Time-of-Flight for Ultrasonic Signal Based on Defect Peaks Tracking Model. Rem Sens. 2023; 15(3): 599. doi: 10.3390/rs15030599.
37. Wan J, Yu Y, Wu Y, Feng R, Yu N. Hierarchical Leak Detection and Localization Method in Natural Gas Pipeline Monitoring Sensor Networks. Sensors. 2012; 12(1): 189-214. doi: 10.3390/s120100189.